J. Fluid Mech. (1977), *vol.* 81, *part* 2, *pp.* 241–256
Printed in Great Britain

The interaction between capillary waves and a current and wave decay

By F. Y. SORRELL AND G. V. STURM†
Department of Mechanical and Aerospace Engineering, North Carolina State University, Raleigh

(Received 10 September 1976 and in revised form 12 January 1977)

Results of experiments on capillary-wave decay and energy transfer to mean currents are presented. The conditions investigated were those of a progressive wave train propagating on still water, on a constant current and on a spatially varying current. The waves were generated by either a mechanical or a pneumatic wave maker and the wave maker usually excited cross-wave motion. Thus the study also provides data on cross-wave generation and growth under these conditions. In particular these results indicate that the cross-waves obtain energy from a constant current as well as a spatially varying current. The progressive-wave energy was separated from that in the cross-waves by spatial averaging. When this is done the wave–current interaction and wave decay can be described by a first-order theory which includes viscous dissipation.

1. Introduction

In dealing with many aspects of air–sea interaction or with remote sensing of the ocean, one is as concerned with the ocean's surface roughness as with the wave height or surface energy distribution. On a wind-ruffled water surface the capillary waves will typically have higher values of ak (a = wave amplitude, k = wavenumber) than the gravity waves, and thus the capillary waves usually make a larger contribution to the ocean's surface roughness than do the gravity waves. An indication of this is given by the larger theoretical values of ak possible before wave breaking for capillary waves or by the more successful theories of radar scattering. These theories are formulated by assuming that the ocean surface is roughened by capillary waves and tilted by gravity waves. This observation has led to an increased interest in and increased study of capillary waves, particularly as they occur on the ocean surface. Such was the motivation of the present work, whose objective was the generation and study of large amplitude capillary waves.

Crapper (1957) predicted the wave profile for finite amplitude capillary waves, and Schooley (1958) demonstrated the existence of this profile with wind-generated capillary waves. However, there apparently have been no published attempts to reproduce this wave profile with either plunger- or flap-type mechanical wave makers. The closest work appears to be that of Gottifredi & Jameson (1970), who produced capillary–gravity waves mechanically and then increased the wave energy by air–water interaction. Although they very successfully achieved a growth of wave energy, only sinusoidal waves were measured and no cross-waves were observed. This observation was possibly due to the large spatial area of their wave measurement probe.

† Present address: University of Tennessee, Knoxville.

The present attempts to use a mechanical wave maker to produce large amplitude capillary waves were totally frustrated by the presence of cross-waves, i.e. waves perpendicular to the wave maker. Cross-wave motion is often observed when a mechanical wave maker is used and thus this problem is not new. McGoldrick (1968) describes an experimental and analytical study of the cross-waves that occurred when capillary–gravity waves were generated by a triangular plunger. Mahony (1972), in an effort to relax a restriction in previous analyses, employed the theory of resonant interactions to study the instability mechanism and thus the generation of gravity cross-waves. Barnard & Pritchard (1972) experimentally confirmed the work of Mahony and their results also agree well with those of McGoldrick.

Of the present experiments, those that were carried out in still water confirm the description given by the above workers. In all cases, a resonably well defined stability margin was observed in that a wave-maker amplitude could be found above which cross-waves were generated and below which no cross-waves were observed. In addition, the energy supplied to the cross-waves appeared to come from the wave maker and rather long (greater than 100 s) oscillations in cross-wave energy were observed. However, as the wave maker was driven at larger and larger amplitudes, the energy went into the cross-waves rather than the progressive waves. Because of this, a progressive wave train could not be generated with a sufficiently large value of ak to produce a finite amplitude wave. Thus it was concluded that it was probably not possible to generate a train of finite amplitude capillary waves with a mechanical wave maker. Consequently, another technique was sought.

The plan chosen was to generate the waves on a water surface in which there was a mean current rather than on a stagnant fluid. The idea was to generate capillary waves with very low cross-wave content and then propagate them into a current in such a manner that they would gain energy by wave–current interaction. It was planned that this technique would supply energy to the progressive waves with no source of energy for the cross-waves. The method was also chosen because of our interest in using wave–current interaction as a method of measuring currents by remote sensing. Three different experimental conditions were investigated: (i) capillary-wave generation on a stagnant fluid, which permitted confirmation of the technique and provided the results previously discussed; (ii) capillary-wave decay with a constant mean current; (iii) the generation and the subsequent decay and energy transfer of capillary waves when they propagate through a region of spatially varying mean current. It should be noted that only in case (iii) is there energy transfer between the progressive waves and the current.

A summary of all of the experimental results is given at the end of the paper; however it is mentioned here that in no case were waves generated with sufficiently large amplitude that first-order theory could not explain the results. Moreover, in many cases there was energy transfer to the cross-waves from the current when there was no energy transfer to the progressive wave train. The paper is divided as follows. Section 2 describes the experimental technique and the results of wave decay measurements without current. The precautions necessary to assure the clean water surface required for capillary-wave experiments is also considered here. The experiments and results for capillary waves on a constant current are described in §3 and §4 describes the experiments and results with a variable current. A summary of all the results and the conclusions drawn from these results is given in §5.

2. Experimental technique

On a water surface without a surface film or contaminant, the damping of surface waves results from viscous energy dissipation in the bulk of the fluid. For a one-dimensional progressive wave train this energy decay can be written as

$$E = E_0 \exp\left[(-4\nu k^2/c_g)\, x\right], \tag{2.1}$$

where ν is the kinematic viscosity, c_g the wave group velocity and x the direction of wave propagation. This is a well established result (e.g. Davis & Vose 1965; Phillips 1966, p. 37) obtained from a first-order wave analysis. The wave energy is

$$E = \rho\sigma^2 a^2/2k, \tag{2.2}$$

where ρ is the fluid density and σ is the radian frequency. In the present experiments the assumption of deep-water waves is completely justified, and thus σ can be expressed in terms of k through the deep-water relationship $\sigma^2 = gk + \gamma k^3$, where g is the acceleration due to gravity and γ the kinematic surface tension T/ρ. Using this expression, (2.2) can be written as

$$E = \frac{\rho(ak)^2\gamma}{2}\left(1 + \frac{g}{\gamma k^2}\right) = \frac{\rho(ak)^2\gamma}{2}(1+\beta), \tag{2.3}$$

where $\beta = g/\gamma k^2$ is a dimensionless term that indicates the relative importance of gravity and surface tension. The term ak is the maximum slope of the wave $\zeta = a\sin(kx - \sigma t)$, i.e. $ak = (d\zeta/dx)_{\max}$; furthermore, it follows that $\frac{1}{2}(ak)^2$ is equivalent to $[(d\zeta/dx)_{\text{r.m.s.}}]^2$, where r.m.s. indicates the root mean square. For capillary waves ($\lambda < 1{\cdot}7$ cm) $\beta < 1$, and $\beta \to 0$ as $\lambda \to 0$. For the short capillary waves characteristic of the present experiments λ is less than 1 cm and β has a maximum of 0·34. Assuming that β can be neglected, (2.3) can be approximated by

$$E \doteq \rho\gamma(d\zeta/dx)^2_{\text{r.m.s.}}, \tag{2.4}$$

and (2.1) can be written as

$$E = \rho\gamma(d\zeta/dx)^2_{0\text{r.m.s.}} \exp\left[(-4\nu k^2/c_g)\, x\right]. \tag{2.5}$$

This means that

$$(d\zeta/dx)_{\text{r.m.s.}} = (d\zeta/dx)_{0\text{r.m.s.}} \exp\left[(-2\nu k^2/c_g)\, x\right]. \tag{2.6}$$

Thus, for short capillary waves, a wave with initial slope $(d\zeta/dx)_0$ will decay at a rate given by

$$\Delta_v = 2\nu k^2/c_g, \tag{2.7}$$

where Δ_v is the viscous logarithmic decrement (attenuation coefficient). The logarithmic decrement is defined as the natural logarithm of the ratio of any two successive wave amplitudes (slopes) divided by the wavelength, i.e. $\Delta = \ln(a_i/a_{i+1})/\lambda$ or simply $\Delta = \ln(2/d_2)$, where d_2 is the distance required for the wave slope to decay to one-half the original value.

Davis & Vose (1965) and McGoldrick (1970) have established the strong dependence of surface tension and wave damping on surface conditions. In addition many other workers have discussed the necessity of a completely clean surface when dealing with capillary waves. Because of this, a number of experiments on capillary-wave decay without a mean current were performed in order to establish the procedure necessary

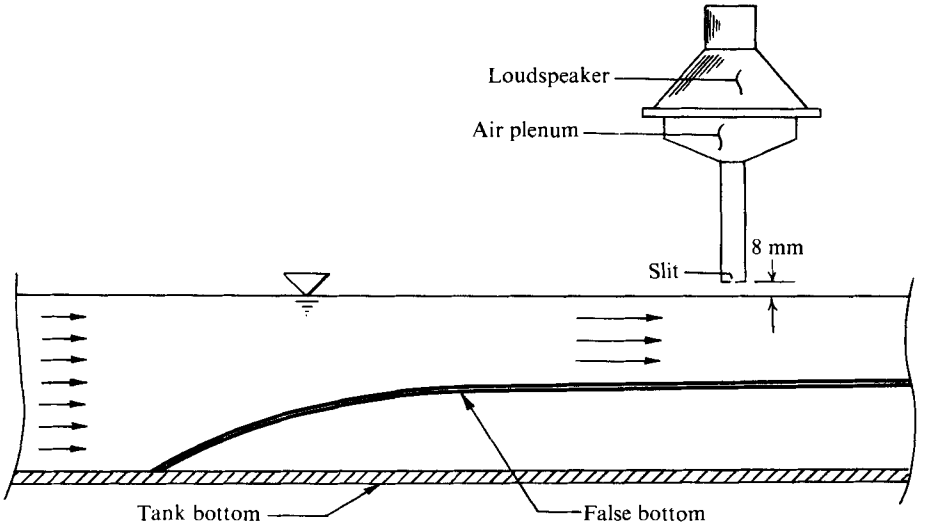

FIGURE 1. Schematic representation of the experimental facility.

to assure a clean water surface and to confirm the experimental technique. The experimental arrangement is described next then a brief summary is given of the zero-current wave decay studies.

All experiments were conducted in a Plexiglas wave tank measuring 256 × 20 × 18 cm. The original wave maker for the system was a 30° triangular plunger whose shaft was driven by a permanent-magnet loudspeaker 15 in. in diameter. The motion of the plunger was monitored by a d.c. differential transformer. However, with mean water currents the mechanical plunger stagnated the flow near the surface and produced a series of ripples which interfered with the capillary waves under study. Because of this, the pulsed-air (pneumatic) wave maker shown in figure 1 was used to generate waves on a current. This device used the previously mentioned loudspeaker with an attached air plenum and duct to produce air pulses. These pulses were directed through a slit 2 mm wide and 20 cm long (the width of the wave tank) located approximately 8 mm above the water surface. Currents were generated, when desired, by use of a recirculating pump and a false tank bottom which produced a test section of reduced area: 20 cm wide and 5 cm deep. Current velocity was measured with a hot-grid probe of the type described by Sorrell & Sturm (1974), used with a constant-temperature bridge.

All data were obtained as follows. The wave slope was determined by an optical slope measuring system previously reported by Sturm & Sorrell (1973). This device uses the refraction of a vertically directed light ray, and does not require any contact with the water surface. Changes in wave slope resulting from small variations in wave amplitude were minimized by averaging over several periods ($n > 10$) with a true r.m.s. voltmeter. The period τ of the wave maker was measured by a digital counter and static surface tension T by a du Nouy tensiometer. The wavelength was measured by placing the wave detector at a fixed position and comparing the wave phase with a reference source (the function generator driving the wave maker). The wave detector was then translated a total of five wavelengths (5λ) by comparing the wave phase with

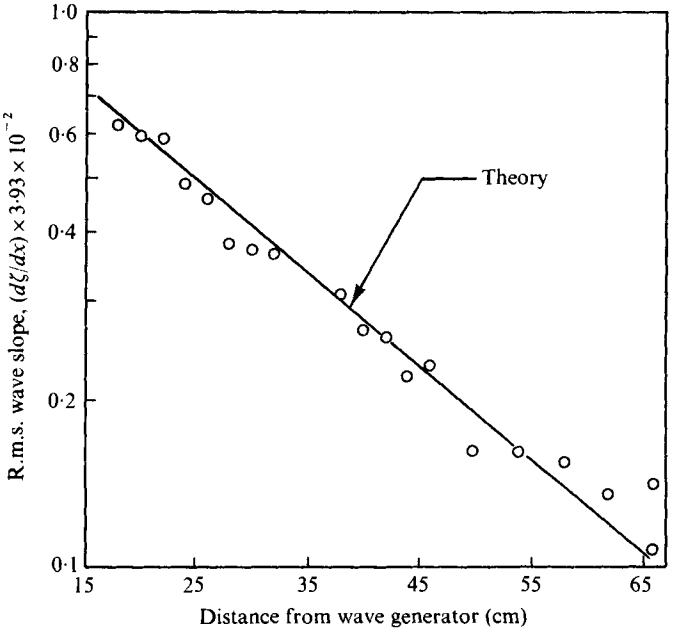

FIGURE 2. The measured decay of capillary waves on a still fluid ($U = 0$). ——, theoretical prediction.

the reference source. The average value of the wavelength was then taken as the actual wavelength. This averaging technique was used to spread the error in determining when exactly 2π radians of phase shift had occurred over five wavelengths. The process is justified because the error in determining the phase shift is greater than any possible change in phase velocity over five wavelengths. The experimental phase velocity c was calculated from $c = \lambda/\tau$ and Δ, the logarithmic decrement, was measured from the slope of the experimental decay data when plotted on a semi-log scale (see figure 2).

The calculated values of the phase velocity c are obtained from

$$c^2 = g/k + \gamma k \tag{2.8}$$

and those of the group velocity c_g from

$$c_g = \tfrac{1}{2}(g + 3\gamma k^2)\,(gk + \gamma k^3)^{-\frac{1}{2}} \tag{2.9}$$

using the static experimental value of the surface tension and the measured wavelength. The wave Reynolds number $R_w = (\sigma/\nu k^2)$ was calculated from the measured wavelength and frequency ($\sigma = 2\pi/\tau$) and tabulated values of viscosity at the measured temperature.

The water surface was constantly skimmed to remove surface film. This was done by adding water to the tank at a rate of approximately 10 cm^3/min and drawing off water at the same rate with a slightly submerged sharp-rimmed standpipe, for all experiments. However, owing to the unpredictable nature of surface films, plus the fact that their presence would greatly alter any results, a check on the presence of surface contaminants was considered desirable. This was accomplished as follows. The damping of surface waves by a rigid (inextensible or closely packed) film gives a logarithmic

decrement $\Delta_f = (\frac{1}{8}\sigma\nu k^2)^{\frac{1}{2}}/c_g$, which is a factor of $2^{-\frac{5}{2}}R_w^{\frac{1}{2}}$ larger than Δ_v, the viscous dissipation decrement.

For all waves with R_w larger than 32, Δ_f is greater than Δ_v. In the present experiments R_w varies between 200 and 350 and Δ_f is a factor of 2·5–3·5 larger than Δ_v. Thus the total decrement Δ_t would be a factor of 3·5–4·5 larger than the viscous dissipation decrement Δ_v. McGoldrick (1970) observed a decay corresponding approximately to the rigid film plus viscous decrement for clean unskimmed tap water.

A number of capillary-wave decay measurements were made to determine the decay decrement experimentally. A typical result is shown in figure 2, which is for a wavelength $\lambda = 0{\cdot}733$ cm in 23 °C tap water. The measured kinematic surface tension was $\gamma = 71{\cdot}3$ cm^3/s^2 and the measured logarithmic decay decrement was $\Delta = 0{\cdot}0378$ cm^{-1}. The wave Reynolds number R_w was 321·6 and the computed viscous decay decrement was $\Delta_v = 0{\cdot}0383$ cm^{-1}. This is a typical result, characteristic of experiments over the complete range of wavelengths, and is considered an adequate indication that the precautions of a clean tank and constant skimming were sufficient to assure that little or no surface film was present. Other experimentalists are cautioned on the necessity of skimming. With the present arrangement, when skimming was stopped for over 5–10 min the waves began to decay at significantly larger decrements. During this period the static kinematic surface tension, as measured by a du Nouy tensiometer, showed only a slight decrease of 1–2 cm^3/s^2. This decrease is so small that it can be easily overlooked; yet the presence of surface contaminants, as indicated by the greatly increased wave damping, is clearly demonstrated.

3. Capillary waves on constant currents

Using the arrangement shown in figure 1, wave decay measurements with constant velocity currents directed against the direction of wave propagation were carried out. The current velocity in the test section was maintained at a constant value to within $\pm 0{\cdot}5$ cm/s (the resolution of the anemometer) and is tabulated with the other data.

In the majority of these trials the cross-wave amplitude increased as one moved away from the wave generator. In addition, the ratio of cross-wave to progressive-wave amplitude remained nearly constant over a wide range of wave-maker amplitudes. In particular no point of neutral stability, as observed without current, could be found. That is, cross-waves were apparently generated whenever progressive waves were generated. Initially, it was reasoned that the pneumatic wave maker could be the cause of these cross-waves. Because it was not possible to use the mechanical wave maker with a current, a comparison of the two wave makers without a current was made. Figure 3, which is a plot of the percentage variation in r.m.s. slope *vs.* distance from the wave generator, presents the results of these experiments. Note that without current the variation in slope due to the cross-waves increases only slightly as one moves away from the wave generator. In absolute terms the cross-waves decay less rapidly than the progressive waves, and thus the percentage cross-wave slope increases initially. However, when one looks at only the cross-mode it shows a monotonic decay. There is a slight difference between the pneumatic and mechanical wave makers, but since they produce nearly equal cross-wave content 15–20 cm from the wave maker, this was not considered the cause of the cross-waves. In addition a wave generator amplitude corresponding to neutral cross-wave stability was also observed

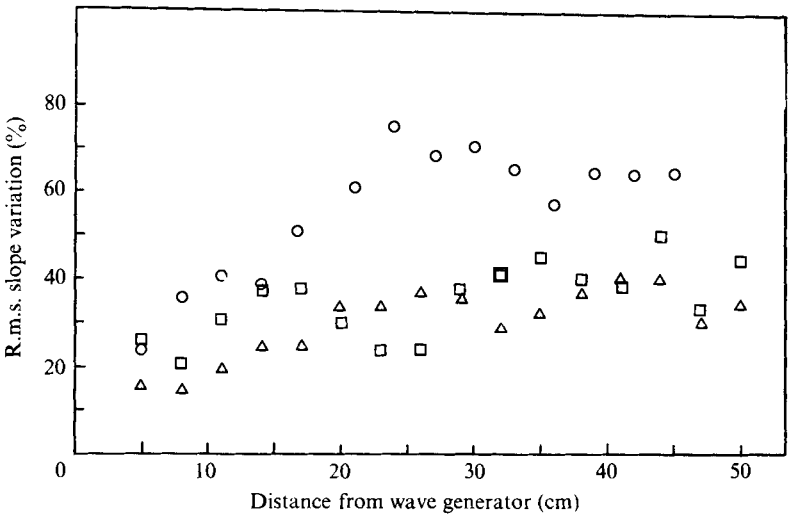

FIGURE 3. Growth of cross-wave content with distance from the wave generator. △, mechanical plunger, no current; ⊡, pneumatic plunger, no current; ○, pneumatic plunger, $U = -8$ cm/s.

with the pneumatic wave maker. This amplitude, however, is not easily compared with that of the mechanical wave generator.

The source of the increased cross-wave energy with a current can be found from the data in figure 3. With a -8 cm/s current the cross-waves actually increase in amplitude as one moves away from the wave generator. By convention, the current is considered negative when it is in a direction opposite to the wave propagation. The actual distribution across the channel is shown in figure 4, which gives plots of the progressive-wave slope across the central 10 cm of the wave channel. Recall that these data were obtained by averaging over a minimum of 10 wave periods; thus they confirm that the cross-waves are indeed standing waves. The wave slope distribution across the channel is given at distances of 5, 11, 17, 24, 36 and 48 cm from the wave generator, and it can be seen that the cross-waves grow or gain energy from the current up to a distance of about 24 cm from the wave generator. After reaching this distance the cross-waves begin to decay. The effect of this uneven wave distribution on the progressive-wave energy (at a single transverse location) is shown in figures 5 and 6. These are plots of the r.m.s. slope of the progressive waves *vs.* distance from the wave generator, and thus the figures are identical with figure 2, but with a -8 cm/s current. Figure 5 shows the measured decay at the centre-line of the test section (10 cm from either wall) and figure 6 gives the same results 1 cm on either side of the centre-line. This is a further indication that the energy is unevenly distributed across the wave tank as one moves away from the wave generator. That this is due only to the cross-waves is rather dramatically illustrated by averaging the r.m.s. wave slope over the width of the tank. In practice this was accomplished by measuring the wave slope as a function of distance from the wave generator at several transverse locations across the tank (symmetrically about the centre-line). The number of transverse locations varied between 5 and 10 with 7 (3 on each side of the centre-line) usually sufficient to average out the cross-motion. If an insufficient number of transverse measurements were made, excessive scatter in the data made it immediately obvious. The tabulated

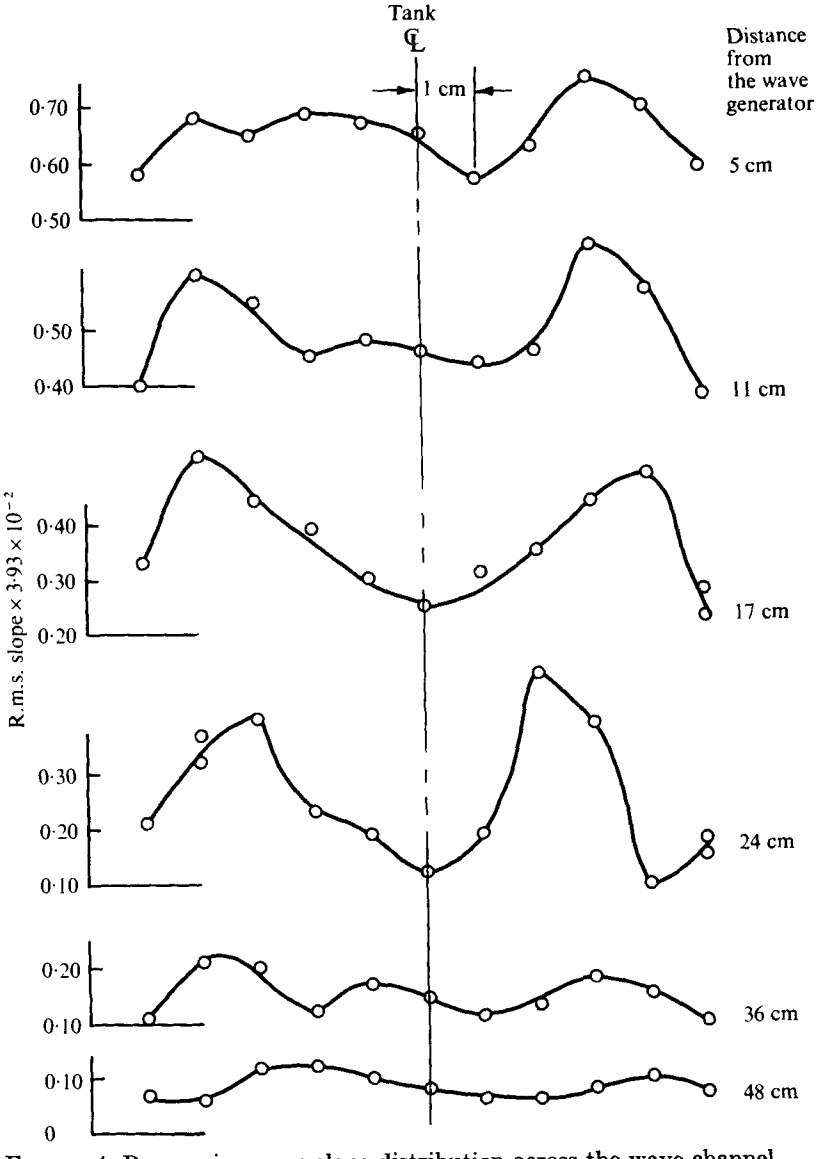

FIGURE 4. Progressive-wave slope distribution across the wave channel.

values for the slope at each position a distance x from the wave generator were then arithmetically averaged to obtain the spatial average across the tank. This was taken as the representative value of the slope, and hence wave energy, for this value of x. The results obtained by using this procedure for the data shown in figures 5 and 6 are given in figure 7. The straight-line (logarithmic) decay rate indicates that the spatial average of the progressive-wave energy decays only by viscous dissipation. A summary of the data for this condition is given in table 1.

The calculated values were obtained in a slightly different manner, which was as follows. Regardless of the cross-wave content, the wave kinematics (wavelength, frequency, current relationship) should obey the equation for conservation of wave

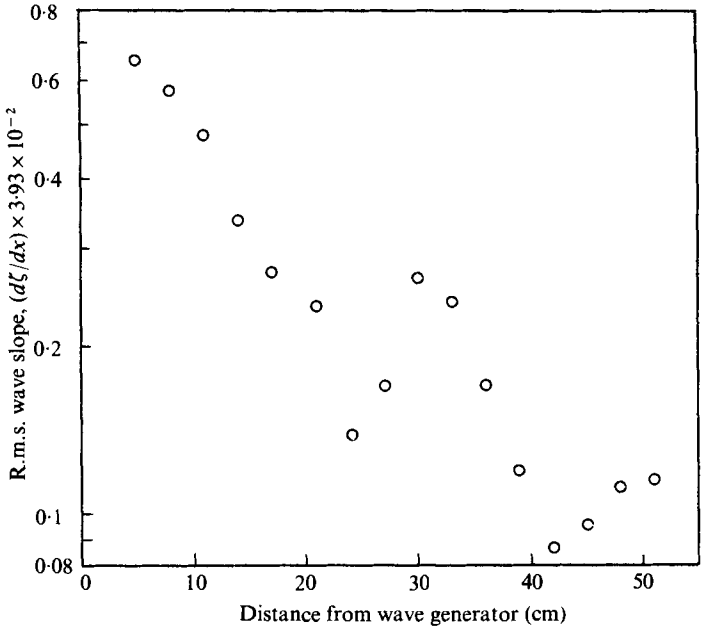

FIGURE 5. The measured decay of capillary waves along the tank centre-line with a current of -8 cm/s.

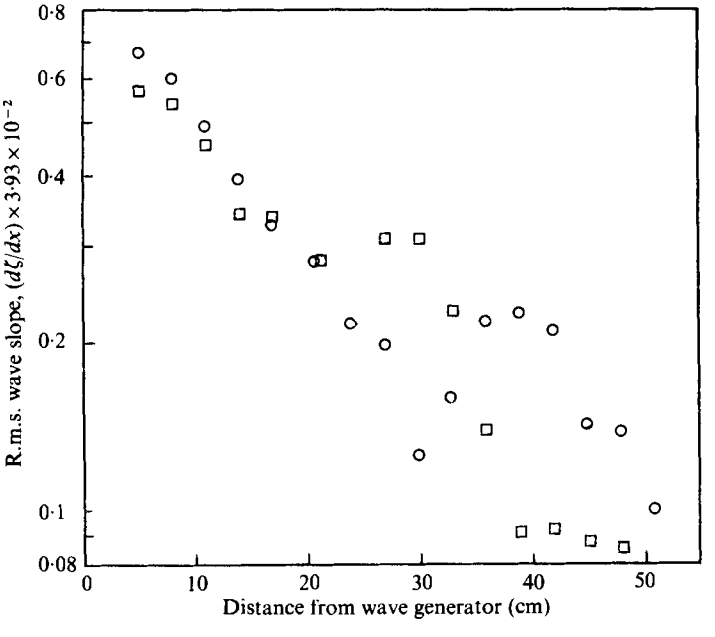

FIGURE 6. The measured decay of capillary waves at 1 cm either side of the tank centre-line with a current of -8 cm/s. ⊙, $+1$ cm from centre-line; □, -1 cm from centre-line.

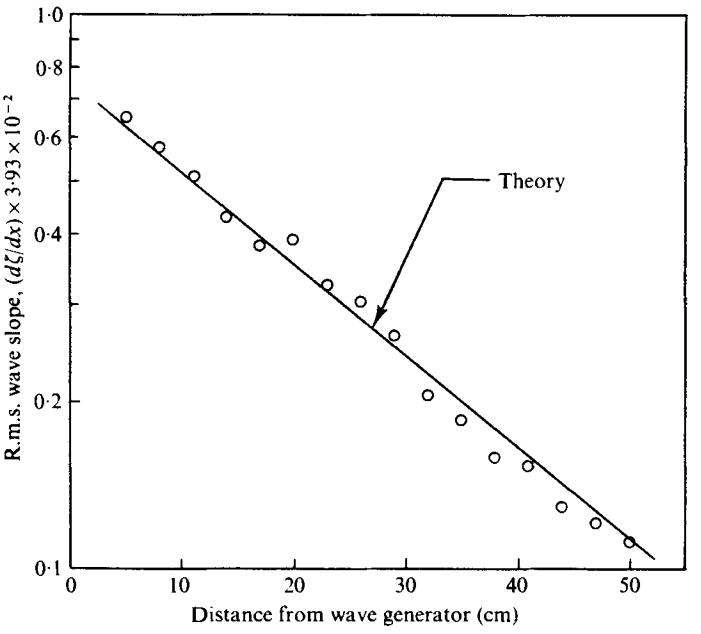

FIGURE 7. Decay of capillary waves on a current of −8 cm/s. The data points are the result of spatially averaging 7 traverses. Figures 5 and 6 are part of the data set.

Measured		Calculated	
T	= 24 °C	R_w	= 264
γ	= 71·4 cm³/s²	Δ_v	= 0·0355 cm^{-1}
λ	= 0·026 cm	d_2	= 19·5 cm
τ	= 54·59 ms	Δ_f/Δ_v	= 2·87
c	= 16·96 cm/s	c_i	= 25·04 cm/s
Δ_{exp}	= 0·038	U	= $c_i - c$ = 8·08 cm/s
U	= 8 cm/s		

TABLE 1. Current and wave parameters for the conditions corresponding to figures 4–7.

phase. A convenient form, given by Phillips (1966, p. 43), for a steady wave field is

$$\eta = \text{constant} = \sigma_0 = \sigma + kU, \tag{3.1}$$

where η is a general wave frequency, U is the mean current and σ_0 is the wave frequency where $U = 0$. This can be written as

$$\sigma_0 = k_0 c_0 = kc = k(c_i + U), \tag{3.2}$$

where k_0 is the wavenumber when $U = 0$ while k is the wavenumber and c the total phase velocity of the wave propagating on a current U. The total phase velocity c corresponds to the sum of the intrinsic phase velocity c_i [i.e. the velocity based on the wavenumber obtained from (2.8)] and the mean current U. In tables 1 and 2 this current is tabulated under two headings: U (measured) and $U = c_i - c$. The former, U (measured), is that obtained experimentally by the hot-film anemometer. The latter U is calculated indirectly from the measured wavelength λ and the wave period τ,

Measured quantities					Calculated	
τ (ms)	λ (cm)	U (cm/s)	c (cm/s)	Δ_{exp} (cm^{-1})	$U = c_t - c$	Δ_v (cm^{-1})
54·694	0·918	8	16·78	0·0384	8·31	0·0362
58·821	0·894	9	15·19	0·0408	10·10	0·0419
58·161	0·869	10	14·95	0·0433	10·55	0·0426
58·161	0·869	10	14·95	0·0495	10·55	0·0426
58·161	0·869	10	14·95	0·0461	10·55	0·0426
58·159	0·825	11	14·19	0·0617	11·70	0·0477
62·171	0·757	14	12·18	0·0630	14·43	0·0622
62·171	0·695	15	11·18	0·0693	16·24	0·0737
66·439	0·90	11	13·54	0·046	11·7	0·0448
66·439	0·90	11	13·54	0·0478	11·7	0·0448
66·439	0·90	11	13·54	0·0468	11·7	0·0448
80·415	0·986	12	12·26	0·0461	12·38	0·041
80·415	0·986	12	12·26	0·0461	12·38	0·041
80·415	0·986	12	12·26	0·0461	12·38	0·041
80·415	0·986	12	12·26	0·0461	12·38	0·041
99·618	1·143	11	11·48	0·0315	12·39	0·0349
99·618	1·143	11	11·48	0·0308	12·39	0·0349

TABLE 2. Summary of constant-current wave kinematics and decay experiments.

where the total phase velocity $c = \lambda/\tau$ and the intrinsic phase velocity is obtained from (2.8), using the local wavenumber $k = 2\pi/\lambda$. The viscous logarithmic decay decrement $\Delta_v = 2\nu k^2/c_g$ is computed using the actual (local) wavenumber and group velocity.

The close agreement between the measured and computed values of U validates the overall experimental technique. The equally close agreement between measured and computed values of the decay decrement Δ again indicates the absence of surface films (for $R_w = 210\Delta_f = 2{\cdot}5\Delta_v$). More dramatic, however, is the observation of energy transfer from the current to the cross-wave mode with no energy transfer to or effect on the progressive wave train. An indication that this is truly a representative result is given in table 2, which is a summary of 17 such experiments. Additional details on these experiments can be found in thesis by Sturm (1973).

4. Capillary waves on variable currents

As previously mentioned, no wave–current interaction is expected unless the progressive waves propagate through a region of spatially varying current. However, the experiments in §3 demonstrate that there is energy transfer to the cross-waves from a constant current. Thus it seemed somewhat unlikely that the original concept of using a variable current to produce a finite amplitude progressive wave train would be successful. However, because the phenomenon was not fully understood, it was not obvious that cross-wave generation and progressive-wave decay and energy transfer would proceed as with the constant current. Therefore experiments on wave–current interaction were undertaken. These experiments required that the capillary waves be generated on a steady current and then propagate into a region where the current is spatially varying. The only practical arrangement with the present experimental system was to generate waves on a negative (opposite to the direction of wave

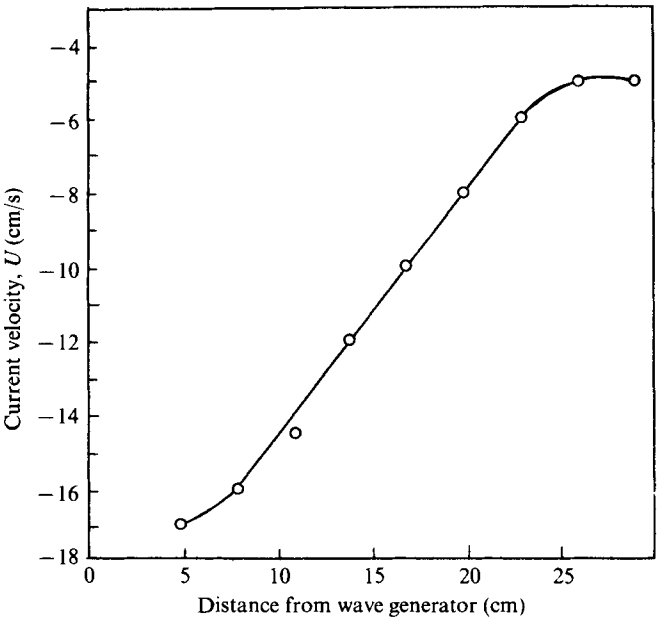

FIGURE 8. Experimentally measured velocity in the variable-current test section.

propagation) current of -17 cm/s and allow the waves to propagate into a region where the current slowly decreased to -5 cm/s. This results in energy transfer from, rather than to, the progressive waves. However, as mentioned, this was about the only experimental arrangement possible; and it did allow an investigation of the cross-wave growth coupled with wave–current interaction.

The current was generated by a variable-area test section and a plot of the current distribution in the test section is given in figure 8. The current was measured by the hot-film probe described in §3, and the magnitude decreases linearly over a region of about 20 cm as one moves away from the generator (located at $x = 0$). Waves with a period of 92·99 ms (10·73 Hz) were generated on the -17 cm/s current; these waves propagated through the variable-current region and were finally dissipated in the -5 cm/s constant-current region. The measurement of capillary-wave decay proceeded in a manner identical to that of the previous constant-current experiments with the exception of wavelength measurements. These were obtained indirectly as follows. Equation (3.3) can be rearranged to yield

$$k^2c_i^2 = k_0^2c_0^2 + k^2U^2 - 2K_0c_0Uk. \tag{4.1}$$

By using the dispersion relation (2.9) with (4.1) one can then solve for the wave-number. This results in a cubic equation of the form

$$(k_0/k)^3 + a_1(k_0/k)^2 + a_2(k_0/k) + a_3 = 0, \tag{4.2}$$

where the coefficients a_1, a_2 and a_3 depend only on the known quantities U, c_0, k_0, γ and g and are given by

$$a_1 = -(2Uc_0 + g/k_0)/c_0^2, \quad a_2 = (U/c_0)^2, \quad a_3 = -\gamma k_0/c_0^2.$$

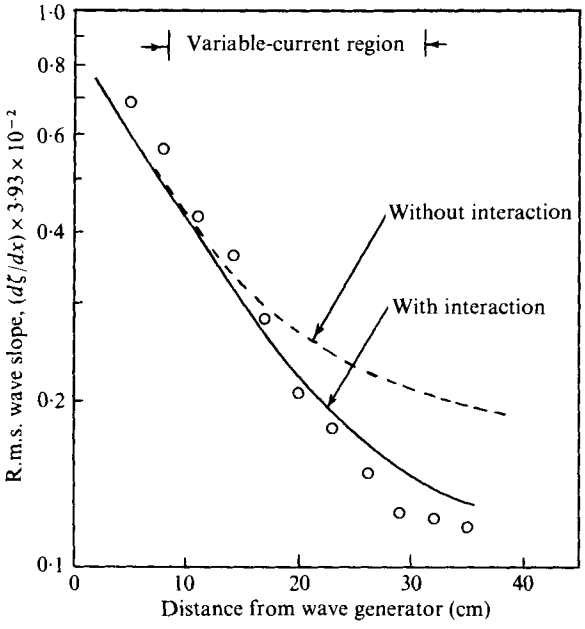

FIGURE 9. Energy transfer and dissipation of capillary waves on the variable current shown in figure 8. ○, spatial average of 7 traverses; – – –, predicted wave decay without wave–current interaction; ——, predicted wave decay including wave–current interaction.

Equation (4.3) is then solved explicitly for k to give an expression of the form

$$k = k(k_0, c_0, U, \gamma, g). \tag{4.3}$$

Therefore, for each value of the current U, one can obtain a corresponding value for k and hence for the wavelength λ. Using this method to determine λ the decay of the waves was measured and is presented in figure 9. These data are spatial averages of seven traverses of the test section, which were necessary because of the cross-waves. Here the cross-waves were observed to gain energy from the current in approximately the same manner as with constant currents.

The expected or predicted decay was also computed for the conditions shown in figure 9. First the decay owing to viscous dissipation alone was computed and is given by the dashed line in the figure. This was obtained by using the measured current and then employing (4.3) to calculate the wavenumber k at each data point. This local wavenumber was used to compute the viscous decay decrement Δ_v at each point. These local values of the decay decrement were then numerically integrated. It can be seen that the initial and final decay rates (slope of the dashed line) are tangential to the data. This is consistent with wave decay on constant currents (which is due only to viscous dissipation) because at either end of the variable-current section approximately constant-current conditions exist.

The effects of the variable current on wave energy through current–wave interaction was computed in a manner suggested by Phillips (1966, p. 49). For a one-dimensional wave train propagating in the x direction, the conservation of the fluctuating component of the wave energy can be expressed as

$$\frac{d}{dx}[E(U+c_g)] + S_{xx}\frac{dU}{dx} = -\epsilon, \tag{4.4}$$

where E is the wave energy, U the current velocity, c_g the wave group velocity, S_{xx} the radiation stress in the x direction, and ϵ the rate of energy dissipation per unit volume due to viscosity. From a first-order analysis, it follows that

$$\epsilon = 2\mu\gamma k^2(ak)^2 = 4\nu k^2 E$$

and

$$S_{xx} = E(3+\beta)/2(1+\beta),$$

where $\beta = g/\gamma' k^2$ is the dimensionless parameter introduced in (2.3). In this experiment β reaches a maximum value of 0·98 and thus the acceleration due to gravity is no longer negligible. In order to provide an approximate analysis, the radiation stress S_{xx} and the group velocity c_g were expanded in a power series with β as an ordering parameter. To first order in β one obtains

$$S_{xx} = E(\tfrac{3}{2}-\beta), \quad c_g = \tfrac{1}{2}(3-\tfrac{1}{2}\beta)c, \tag{4.5}$$

and with this approximation (4.4) can be rewritten as

$$dE/dx + p(x)E = 0, \tag{4.6}$$

where

$$p(x) = \left[(\tfrac{5}{2}-\beta)\frac{dU}{dx} + (\tfrac{3}{2}-\tfrac{1}{4}\beta)\frac{dc}{dx} + 4\nu k^2\right]/[U + (\tfrac{3}{2}-\tfrac{1}{4}\beta)c]. \tag{4.7}$$

Equation (4.6) has a general solution of the form

$$E = E_0 \exp\left[-\int_0^x p(\omega)\,d\omega\right], \tag{4.8}$$

where E_0 is the wave energy at $x = 0$ and $p(x)$ can be thought of as a generalized decay coefficient. In the limit of a constant current dU/dx and dc/dx are zero, and $p(x)$ reduces to $4\nu k^2/c_g$ as obtained in (2.1).

With a variable current $p(x)$ is a function of $U(x)$, which must be determined from experimental measurements. In view of the difficulty in obtaining a compact functional form for $p(x)$, no closed-form integration of (4.8) was attempted. Rather, a simple graphical integration was employed in order to produce a table of values for the definite integral

$$\int_0^x p(\omega)\,d\omega.$$

Subsequently, E/E_0 was evaluated from (4.8) at each data point and plotted on a semi-logarithmic scale. Within a constant, the result of this calculation is presented as the solid line in figure 9. The computed decay agrees with the data reasonably well, except in the low current region. This is probably due to β becoming so large that terms of order greater than one in β are needed. In view of the many approximations and the somewhat crude analysis the agreement between the theory and the experiments is considered quite satisfactory.

The experiments indicate that the progressive waves do interact with the current as predicted by first-order analysis. This occurs in the presence of large amplitude (or slope) cross-waves which are also interacting with the current. In addition the flow straighteners upstream of the test section appear to produce some cross-wave or generally random wave motion that is propagated into the upstream end of the test section. Therefore, even in the presence of cross-waves or other superfluous wave

motion of greater amplitude, the progressive wave train interacts only with the current. As matter of interest the initial wave decay in the high current region is primarily due to viscous dissipation, while at the lower currents the energy decay is largely from wave–current interaction. This can be seen by a comparison of the total energy decay (solid line) with that due to viscous dissipation alone (dashed line). A comprehensive analysis of the interaction of capillary–gravity waves with currents, but without viscous dissipation, has recently been given by Huang (1974). As long as viscous dissipation does not completely dominate the interaction, this analysis is of considerable help in understanding wave–current energy dynamics.

5. Summary and conclusions

Owing to the presence of cross-wave modes it is not very likely that a finite amplitude train of capillary waves can be produced by either plunger- or flap-type wave makers. This is because the cross-waves sap most of the energy that the wave maker is supplying to the water surface. Moreover, while the motion of cross-waves on a still fluid is moderately well described by existing theory and confirmed by experiments, their generation and growth in the presence of a mean current is not very well understood. In particular, these experiments indicate that the cross-waves gain energy from the current. This source of energy for cross-wave modes makes it even more difficult to generate a well-defined finite amplitude progressive train of capillary waves on a current. The large amplitude cross-waves present with a current make for a rather uneven distribution of wave energy across the tank, and thus spatial averaging of the progressive wave train is usually required. However, with spatial averaging in a direction perpendicular to that of wave propagation, the wave decay due to viscous dissipation and the energy transfer due to wave–current interaction proceed according to one-dimensional first-order theory.

Finally, there must be some concern about the validity of any studies of one-dimensional wave–current interaction. These experiments indicate that with a current cross-wave modes will almost certainly be excited, and that as much energy and energy transfer will be associated with the cross-waves as with the progressive waves. While, as with these experiments, it may be possible to isolate the progressive waves from the cross-modes, it is questionable whether this provides a valid description of the overall surface energy dissipation and transfer. It may well be that a stochastic representation of the water surface is required to provide a complete description of the transfer of surface wave energy to and from the current.

The authors gratefully acknowledge many helpful discussions with Dr N. E. Huang both on the theory of wave–current interaction and on cross-waves. The assistance of Professor L. F. McGoldrick with the analysis of some of the initial cross-wave motion is also acknowledged. This work was supported in part by the National Aeronautics and Space Administration, Wallops Flight Center, through contracts NAS6-2135 and NAS6-2307.

REFERENCES

BARNARD, B. J. S. & PRITCHARD, W. G. 1972 Cross-waves. Part 2. *J. Fluid Mech.* **55**, 245.

CRAPPER, G. D. 1957 An exact solution for progressive capillary waves of arbitrary amplitude. *J. Fluid Mech.* **2**, 532.

DAVIES, J. T. & VOSE, R. W. 1965 On the damping of capillary waves by surface films. *Proc. Roy. Soc.* A **286**, 218.

GOTTIFREDI, J. C. & JAMESON, G. J. 1970 The growth of short waves on liquid surfaces under the action of a wind. *Proc. Roy. Soc.* A **319**, 373.

HUANG, N. E. 1974 Ocean dynamics studies. *N.A.S.A. Contractor Rep.* CR-137467.

MCGOLDRICK, L. F. 1968 Faraday waves: the cross-wave resonant instability. *Univ. Chicago, Dept. Geophys. Sci. Tech. Rep.* no. 2.

MCGOLDRICK, L. F. 1970 An experiment on second-order capillary gravity resonant wave interactions. *J. Fluid Mech.* **40**, 251.

MAHONY, J. J. 1972 Cross-waves. Part 1. *J. Fluid Mech.* **55**, 229.

PHILLIPS, O. M. 1966 *The Dynamics of the Upper Ocean.* Cambridge University Press.

SCHOOLEY, A. H. 1958 Profiles of wind-created water waves in the capillary–gravity transition region. *J. Mar. Res.* **16**, 100.

SORRELL, F. Y. & STURM, G. V. 1974 An alternate to hot film flow sensors. *Rev. Sci. Instr.* **45**, 300.

STURM, G. V. 1973 Experimental studies of capillary waves on currents. Ph.D. thesis, N.C. State University, Rayleigh. Univ. Microfilm, Ann Arbor, Michigan.

STURM, G. V. & SORRELL, F. Y. 1973 Optical wave measurement technique and experimental comparison with conventional wave height probes. *Appl. Optics* **12**, 1928.